Measuring Kinetic Isotope Effects in Enzyme Reactions Using Time–Resolved Electrospray Mass Spectrometry

ARTICLE *in* ANALYTICAL CHEMISTRY · MARCH 2013

Impact Factor: 5.64 · DOI: 10.1021/ac400191t · Source: PubMed

4 AUTHORS, INCLUDING:

Peter Liuni
York University
9 PUBLICATIONS **89** CITATIONS
SEE PROFILE

Ekaterina Olkhov-Mitsel
Samuel Lunenfeld Research Institute
15 PUBLICATIONS **68** CITATIONS
SEE PROFILE

Derek J Wilson
York University
38 PUBLICATIONS **560** CITATIONS
SEE PROFILE

analytical chemistry

Article

pubs.acs.org/ac

Measuring Kinetic Isotope Effects in Enzyme Reactions Using Time-Resolved Electrospray Mass Spectrometry

Peter Liuni, Ekaterina Olkhov-Mitsel,[§] Arturo Orellana, and Derek J. Wilson*

Department of Chemistry, York University, Toronto, ON, M3J 1P3, Canada

Supporting Information

ABSTRACT: Kinetic isotope effect (KIE) measurements are a powerful tool for studying enzyme mechanisms; they can provide insights into microscopic catalytic processes and even structural constraints for transition states. However, KIEs have not come into widespread use in enzymology, due in large part to the requirement for prohibitively cumbersome experimental procedures and daunting analytical frameworks. In this work, we introduce time-resolved electrospray ionization mass spectrometry (TRESI-MS) as a straightforward, precise, and inexpensive method for measuring KIEs. Neither radioisotopes nor large amounts of material are needed and kinetic measurements for isotopically "labeled" and "unlabeled" species are acquired simultaneously in a single "competitive" assay. The approach is demonstrated first using a relatively large isotope effect associated with yeast alcohol dehydrogenase (YADH) catalyzed oxidation of ethanol. The measured macroscopic KIE of 2.19 ± 0.05 is consistent with comparable measurements in the literature but cannot be interpreted in a way that provides insights into isotope effects in individual microscopic steps. To demonstrate the ability of TRESI-MS to directly measure intrinsic KIEs and to characterize the precision of the technique, we measure a much smaller $^{12}C/^{13}C$ KIE associated specifically with presteady state acylation of chymotrypsin during hydrolysis of an ester substrate.

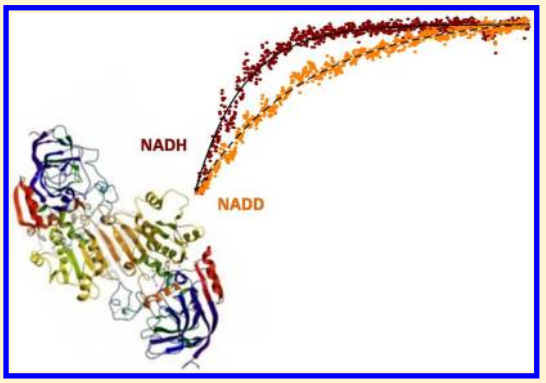

Kinetic isotope effects (KIEs) have a broad range of uses in the study of enzyme mechanisms, providing insights that cannot be obtained by other techniques.[1−4] KIEs have been employed to determine rate limiting microscopic steps,[5−7] link catalysis to dynamics in the active site,[8−11] and structurally characterize transition states.[12−14] However, in spite of their obvious usefulness and a long history development, KIE measurements have not come into widespread use in the broader field of enzymology. There are a number of potential reasons for this, including analytical frameworks that can appear quite daunting even for moderately complex reaction mechanisms, and the ambiguity arises from drawing conclusions about microscopic processes from what are usually steady state measurements.[15,16] This is in addition to the experimental procedure themselves, which are often arduous and expensive.

Scintillation counting was initially the dominant method for measuring KIEs, but the requirement for radioisotopes has resulted in a marked decrease in use. Currently, radiolabeling is used mainly for hydrogen tunneling analyses that compare $^{1}H/^{3}H$ and $^{2}H/^{3}H$ isotope effects, as well as competitive assays for heavy atom KIEs.[17] The majority of KIE measurements are made using optical techniques, but this has severely limited the subset of systems studied due to the requirement for a chromophoric change on turnover. For example, $NAD(P)^{+}$ dependent enzymes represent the overwhelming majority of KIE studies in the literature, partly because of the large isotope effects associated with hydride transfer and a well justified interest in hydrogen tunneling but also because reduction/oxidation of the nicotinate moiety is optically detectable (NADH has a characteristic absorption band at λ = 340 nm).[6,18−20] Optical analysis by UV/visible absorption or fluorescence also generally precludes competitive assays, since isotopically "labeled" and "unlabeled" species are indistinguishable. More recently, MS- and NMR-based methods have emerged that address these limitations somewhat.[21,22] NMR approaches that allow for the measurement of KIEs from natural abundance ^{13}C are especially promising since they do not require isotopic labeling.[23−25] However, these techniques bring their own drawbacks which can include the requirement for a large amount of material,[23,25] limited applicability, and lower precision quantitation of reactants and products.

The ability to distinguish multiple isotopes simultaneously at high sensitivity makes mass spectrometry well suited to the study of isotope effects, as exemplified by the well-established field of isotope ratio mass spectrometry.[26] MS-based approaches have been used to measure KIEs in enzyme systems, typically by quenching the reaction midphase and noting the relative quantities of specifically labeled and unlabeled product.[21,22] This approach is in principle broadly

Received: January 18, 2013
Accepted: March 5, 2013
Published: March 5, 2013

applicable but relies on a single time-point measurement and numerous sample handling steps between quenching and analysis, which can make it difficult to achieve the needed level of precision.

In this work, we introduce a new, straightforward approach for measuring KIEs based on time-resolved electrospray ionization mass spectrometry (TRESI-MS). TRESI-MS is an electrospray-coupled rapid mixing technique that enables monitoring of solution phase processes on the ms time scale.[27] The data are analogous to conventional stopped-flow intensity−time profiles except that no chromophore is required and isotopically labeled and unlabeled species are distinguishable by mass. To establish the feasibility of the approach, we first measure a large, well-studied KIE in the yeast alcohol dehydrogenase (YADH)-catalyzed hydride transfer from ethanol to NAD^+. We then test the limits of the technique by measuring a small $^{12}C/^{13}C$ isotope effect associated with the presteady state acylation of chymotrypsin by the ester substrate para-nitrophenyl acetate (pNPA).

EXPERIMENTAL SECTION

Materials. α-Chymotrypsin, yeast alcohol dehydrogenase, β-nicotinamide adenine dinucleotide, ammonium hydroxide, ammonium acetate, and 4-nitrophenol acetate (p-NPA) were obtained from Sigma-Aldrich (St. Louis, MO). Deuterium oxide, 1,1′-^{13}C acetic anhydride (99%), and 1,1-D_2 ethanol were purchased from Cambridge Isotope Laboratories (Andover, MA). HPLC-grade methanol, ethanol, acetonitrile, and hydrochloric acid were purchased from Caledon Laboratories (Georgetown, ON, Canada). Ultrapure water was generated from the in-house Milli-Q system (EMD Millipore, Billerica, MA). All solutions were pH adjusted using the S20 SevenEasy pH meter (Denver Instruments, Bohemia, NY). For all experiments, infusion and continuous pullback of the inner capillary was conducted using Harvard 11+ infusion syringe pumps (Holliston, MA, USA).

Synthesis of ^{13}C-Labeled pNPA. To a solution of *p*-nitrophenol (1.0 equiv.) in freshly distilled dichloromethane was added a catalytic amount of dimethylaminopyridine (0.05 equiv.) in one portion, followed by a slight excess of acetic anhydride (1.05 equiv.). The reaction was monitored by thin-layer chromatography (TLC) analysis. Once complete, the reaction was diluted with diethyl ether and extracted with water. The ether layer was washed with brine, dried with $MgSO_4$, and concentrated under vacuum. The crude material was purified by column chromatography using silica gel. The final product was characterized by mass spectrometry and UV−vis spectroscopy. ^{13}C-labeled labeled *p*-nitrophenyl acetate was prepared using the same procedure and using 1,1′-^{13}C2-labeled acetic anhydride.

TRESI-MS. Time-resolved measurements were carried out using an electrospray mass spectrometry-coupled capillary mixer described previously (Figure 1).[27,28] Briefly, the device is based on a concentric capillary design. In both YADH and chymotrypsin experiments, the enzyme solution was injected through the polyimide-coated fused silica inner capillary (Polymicro, Pheonix, AZ). Solutions containing 50% labeled and unlabeled substrate were injected through the stainless steel outer capillary (Small Parts, Logansport, IN). Mixing occurred when enzyme solution was released into the intercapillary space from a notch cut 2 mm from the inner capillary end, with the mixed solution then passing into a delay volume. Reaction profiles were acquired by steadily moving the inner capillary back from the end of the outer capillary, resulting in the acquisition of steadily later reaction times. For chymotrypsin experiments, an additional static mixer was added to the end of the outer capillary in order to supply an electrospray-enhancing "makeup solvent" consisting of 10% (v/v) methanol and 6 mM HCl (pH 2) in water immediately prior to ionization. Kinetics were measured from 42 ms to 22 s of reaction time, corresponding to 30 min of inner capillary withdrawal and data acquisition.

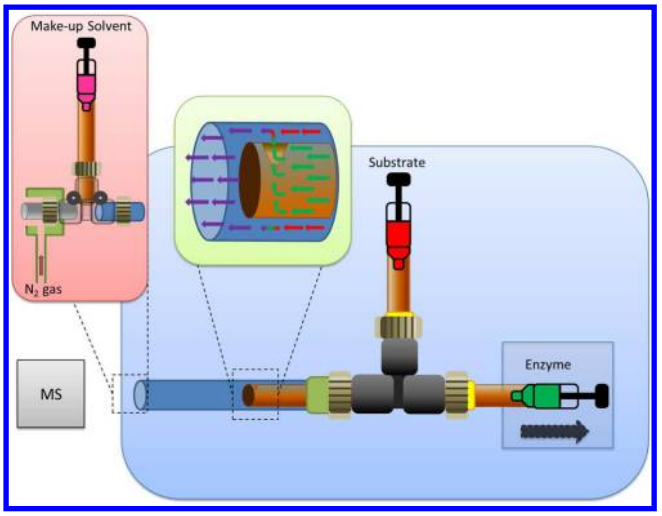

Figure 1. Schematic depiction of the TRESI-MS source.[27] Solution containing enzyme is injected into the "inner capillary" from Syringe 1 (green) via infusion pump. This pump, Syringe 1, and the inner capillary comprise an assembly that can be withdrawn from the source region (gray arrow), resulting in withdrawal of the inner capillary from the end of the outer capillary and a correspondingly increased delay between mixing and ionization. Syringe 2 (red) injects substrate solution through the annular intercapillary space. Mixing occurs when solution from the inner capillary flows into the intercapillary space though a notch cut 2 mm from the end of the inner capillary. Freshly mixed solution then passes into a delay volume which is determined by the position of the inner capillary within the outer capillary and then into a static mixer where electrospray-enhancing "makeup solvent" is added (pink syringe) immediately prior to the onset of ESI.

KIE Measurements. For all experiments, isotopically labeled and unlabeled substrates were mixed and reacted simultaneously in an internal competition assay. In alcohol dehydrogenase experiments, Syringe 1 contained a 2 μM solution of YADH in 10 mM ammonium acetate (pH 8.4). This was mixed with a series of equimolar ethanol and 1,1-D_2 ethanol solutions, (10 mM-200 mM) each containing 400 μM NAD^+ prepared in 10 mM ammonium acetate (pH 8.4). Samples were injected at a total flow rate of 3.0 μL/min. The intensity of NADH and NADD at 666 m/z and 667 m/z, respectively, was monitored as a function of time, and kinetic data was acquired from extracted ion currents at their respective masses. For the purpose of extracting V_0, the 667 m/z signal was assumed to contain a 20% component from NADH due to the M + 1 isotopic peak.

For chymotrypsin experiments, a 25 μM chymotrypsin solution at pH 8.4 is loaded into Syringe 1. A solution containing both 2.5 mM ^{12}C-p-NPA and 2.5 mM ^{13}C-p-NPA was prepared in 40% methanol, adjusted to pH 7.0, and loaded into Syringe 2. A 6 mM HCl solution in 10% methanol is loaded into Syringe 3 as a makeup solvent. Samples were injected at flow rates of 3.5 μL/min for all 3 syringes (10.5 μL/

dx.doi.org/10.1021/ac400191t | Anal. Chem. 2013, 85, 3758−3764

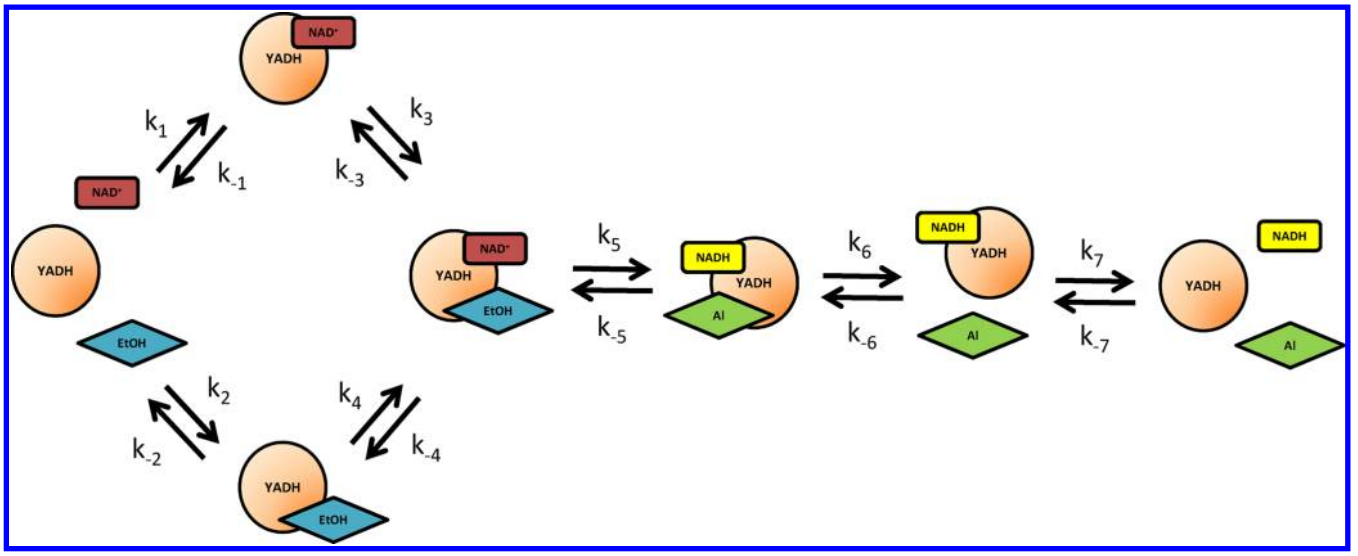

Figure 2. Schematic depiction of the semisequential bi-bi YADH mechanism proposed by Dickinson and Monger in 1973, with release of NADH being the rate-limiting process in the oxidation of ethanol (EtOH) to acetaldehyde (Al).

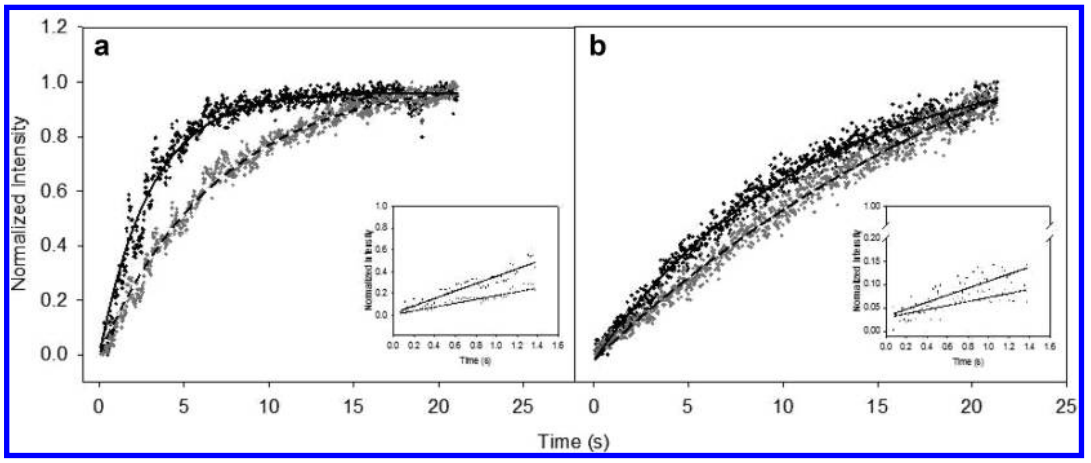

Figure 3. Reaction progress curves for the oxidation of ethanol by YADH at two different ethanol concentrations (a) 200 mM and (b) 10 mM, acquired by monitoring the accumulation of NAD(H/D). Dark circles represent the NADH signal intensity, while gray circles correspond to NADD. Lines are single exponential fits to the data to aid visualization (not used in the analysis). Insets show the linear portions of the progress curves used for the extraction of V_0.

min total flow rate). The makeup solvent also acts as a chemical quencher for the reaction; therefore, the dead time for the mixing tee is negligible. Extracted ion current profiles from peaks corresponding to the 12+, 11+, 10+, and 9+ charge states of the free and acyl-enzyme forms of chymotrypsin, respectively, were acquired and used in the calculation of KIEs.

All experiments were conducted with mild-moderate declustering potentials on a QSTAR Elite Qq-TOF mass spectrometer (AB Sciex, Framingham, MA). ESI voltages were optimized between +4500 and +5500 V (positive ion mode) prior to the acquisition of data. The Analyst QS 2.0 software package was used to control, acquire, and view mass spectral information, and protein mass spectra were deconvoluted using the BioAnalyst software suite (AB Sciex, Framingham, MA).

RESULTS AND DISCUSSION

Yeast Alcohol Dehydrogenase Oxidation of Ethanol. KIEs associated with hydride transfer are among the most well-studied isotope effects, serving as a model for hydrogen tunneling[29−31] and catalysis-linked dynamics.[32,33] The YADH-catalyzed hydride transfer from benzyl alcohol to NAD^+ was the first reaction in which evidence of hydrogen tunneling was reported.[31] There remains nonetheless substantial disagreement on the extent to which hydrogen tunneling can be inferred from the conventional approach of characterizing the pressure or temperature dependence of the KIE.[34] The reliability of KIE-based evidence for the contribution of enzyme dynamics to catalysis has also recently come into question.[16] In the case of YADH, much of the difficulty in interpreting the hydride transfer primary KIE arises from ambiguities in our understanding of the mechanism. Recent studies generally assume the semisequential bi-bi mechanism proposed by Dickinson and Monger in 1973 (Figure 2), with the rate limiting step in the "oxidation-of-alcohol" direction being release of the nucleotide product.[35]

YADH has frequently been used as a protein complex standard for electrospray mass spectrometry.[36,37] Under optimal electrospray conditions, the YADH spectrum is dominated by the intact tetramer, shown in Figure S1, Supporting Information. The addition of saturating concen-

dx.doi.org/10.1021/ac400191t | Anal. Chem. 2013, 85, 3758−3764

trations of ethanol has little impact on the quality of the spectrum, and specific binding to the tetramer is detected via a 184 Da mass shift (i.e., 1 molecule per active site). However, mM concentrations of NAD^+ have a strongly deleterious effect on spectral quality, eliminating the possibility of directly monitoring active enzyme complexes in the steady state. Kinetic measurements were therefore carried out by monitoring the product NAD(H/D), with adjustment to the extracted parameters for the ~20% contribution of the NADH M + 1 (^{13}C) peak to the monoisotopic NADD peak. Typical reaction progress curves from competition experiments involving 50% labeled ethanol (CH_3CD_2OH) at 10 mM (a) and 200 mM (b) are shown in Figure 3. The insets show the linear portions of the curves used to extract initial velocities V_0 for a steady state analysis.

As expected, these data show a significant KIE, with hydride transfer from the labeled ethanol to form NADD being substantially slower than the formation of NADH from the unlabeled substrate. The average "observed" kinetic isotope effect KIE_{obs} extracted directly from these data is $V_{0(NADH)}/V_{0(NADD)}$ = 1.8 ± 0.4; however, this analysis assumes that the isotopic substitution has no influence on any microscopic process apart from the "rate limiting" step, which seems unlikely given that hydride transfer (where the isotopic substitution generates a primary KIE) is not rate limiting.[38] The observed KIE is therefore a macroscopic phenomenon which is better defined in terms of the apparent specificity constant: $KIE_{spec} = (k_{cat(NADH)}/K_{M(NADH)})/(k_{cat(NADD)}/K_{M(NADD)})$, usually abbreviated as $^{D}(V/K)$.[15]

Michealis–Menten plots showing the initial rates of formation of NADH and NADD as a function of ethanol concentration are provided in Figure 4. With the NAD^+ concentration held constant at a saturating level of 20 mM, the V_0 vs. [ethanol] profile exhibits classical Michealis–Menten saturation kinetics. Extracted values of k_{cat} and K_M yield a KIE_{spec} of 2.19 ± 0.05 (R^2 NADH = 0.82, R^2 NADD = 0.88), which is in line with comparable literature values, including the initial measurement by Mahler and Douglas[2] and more recent work by Park et al.[39] The significant difference between KIE_{obs} and KIE_{spec} suggests a substantial shift in one or more microscopic equilibria upon isotopic substitution, but the YADH mechanism is too complex to allow for the determination of specifically which processes are affected from a single macroscopic measurement. Moreover, there are a number of other factors that complicate any attempt at a quantitative interpretation of the observed KIE, in particular an undefined 2° KIE from the deuterium that is not transferred and an untested assumption that catalysis at each active site is fully independent. Random binding of labeled and unlabeled substrate at each active site generates a heterogeneous set of active enzyme complexes, which could distort the observed KIE if the activity of one site is influenced by the activity of another.

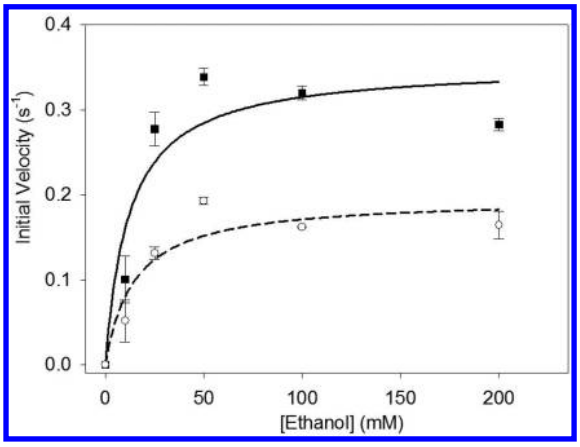

Figure 4. Steady state analysis of YADH catalyzed oxidation of ethanol. Filled squares represent the initial velocities of NADH production, and open circles indicate the same for NADD. After fitting to the Michealis–Menten equation, the data yield a $^{D}(V/K)$ value of 2.19 ± 0.05. Error bars are from 5 replicates.

It is worth noting that some of this ambiguity arises from an inability to directly detect enzyme complexes that are populated in the steady state (i.e., the E·NAD(H/D) complex, where E = enzyme) or the presteady state (e.g., the ternary $E{\cdot}NAD^+{\cdot}CH_3C(H/D)_2OH$ complex). In the case of YADH, the detection of active enzyme complexes is complicated by the presence of NAD^+ as discussed earlier; however, this challenge may prove surmountable with careful adjustment of solvent and ionization conditions. The challenge of distinguishing labeled from unlabeled complexes in competition experiments, on the other hand (i.e., a 2–8 Da difference on a roughly 148 kDa complex), would be daunting even on an ultrahigh resolution instrument. Nonetheless, for smaller proteins, direct measurement of microscopic KIEs via enzyme complex intermediates is possible using TRESI-MS, as demonstrated in the following section.

Primary $^{12}C/^{13}C$ KIE in Chymotrypsin Acylation. In contrast to KIEs involving isotopes of protium, heavy atom KIEs rarely exceed more than a few percent and are therefore much more challenging to measure in terms of achieving the necessary level of precision. Chymotrypsin catalyzed hydrolysis of para-nitrophenyl acetate (mechanism shown in Figure S3, Supporting Information) is among the relatively few enzymatic reactions for which a heavy atom KIE has been reported.[40] This reaction also includes an observable presteady state characterized by the population of an acyl-enzyme intermediate. Acylation of the enzyme is fully rate limiting in the presteady state, and isotopic substitution at the carbonyl carbon has no impact on the substrate binding equilibrium.[40] The primary $^{12}C/^{13}C$ KIE associated with acyl-enzyme formation is therefore attributable specifically to the irreversible acylation step.

The release of chromophoric para-nitrophenolate upon acylation makes the chymotrypsin/p-NPA presteady state accessible to optical analysis; however, the optical equivalency of labeled and unlabeled para-nitrophenol rules out a competition approach for measuring KIEs. By TRESI-MS, presteady state acylation of chymotrypsin is monitored by direct detection of the acyl-enzyme intermediate.[28] Competition experiments are therefore possible in principle but will require the differentiation of a 1 Da difference on a 25 kDa protein, complicated still further by overlapping natural abundance ^{13}C isotope distributions. In terms of fwhm resolution, this requirement is well beyond the capabilities of a typical Q-TOF instrument; however, a competitive KIE can still be measured provided that the "labeled" and "unlabeled" peaks are distinguishable and the extent of overlap between the peaks is known. To determine if the labeled and unlabeled enzyme complex were distinguishable, we collected mass spectra of chymotrypsin in the presence of unlabeled (Figure 5a) and labeled substrate (Figure 5b). In both cases, the free enzyme appears at 25446 ± 2 Da after deconvolution, corresponding to the δ' form of the enzyme.[28] The mass of

dx.doi.org/10.1021/ac400191t | Anal. Chem. 2013, 85, 3758–3764

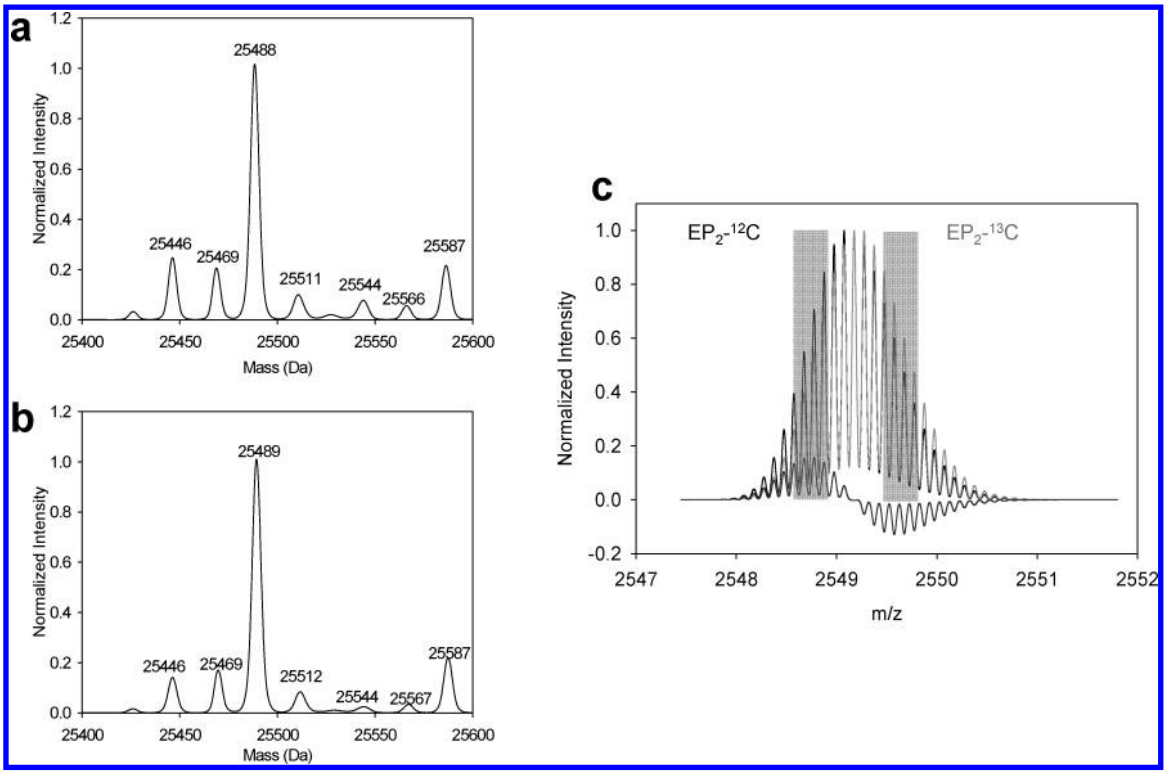

Figure 5. Matched pair of deconvoluted mass distributions for labeled and unlabeled acyl-chymotrypsin. (a) unlabeled; (b) labeled. The peak at 25 446 Da corresponds to free δ′-chymotrypsin while the acyl-enzyme is observed at 25 488 Da in the case of the unlabeled substrate and 25 489 Da in the case of the labeled substrate. The spectra also include a number of sodium and potassium adducts common in commercially supplied samples. (c) A model of the 10^+ m/z peak for labeled and unlabeled acyl-chymotrypsin (50/50 mixture) illustrating the challenge of differentiating the two peaks at the m/z level due to overlap. Peaks for ^{12}C are shown in black, while the ^{13}C peaks are shown in gray. Small peaks appearing above and below the m/z axis are difference peaks ($^{12}C-^{13}C$). Gray areas indicate the ion current extraction window for ^{12}C acyl-enzyme (left) and ^{13}C acyl-enzyme (right), resulting in a 60% contribution from the desired species.

the acyl-enzyme, however, was 25488 ± 3 Da for the unlabeled substrate and 25489 ± 3 Da for the labeled substrate. In terms of absolute mass, these values are identical to within error; however, in each matched set of measurements (n = 5), acylation with labeled substrate resulted in a mass difference that was *always* 1 Da more than acylation with unlabeled substrate. This is a testament to the power of deconvolution over multiple peaks to measure mass *differences* in the absence of an internal standard, and it confirms that there is a measurable difference in peak position between labeled and unlabeled acyl-chymotrypsin.

The challenge in differentiating the labeled and unlabeled acyl-enzyme in individual m/z peaks is illustrated in Figure 5c, in which the labeled and unlabeled 10^+ peaks are modeled at 100 000 fwhm. Kinetics taken from overlapping regions of the distribution will yield a weighted average rate for the two species (see Supporting Information). It is therefore desirable to acquire kinetics from regions of the peak where overlap is lowest, corresponding to the outer edges of the distribution. However, this must be balanced with the need for sufficient signal-to-noise. Ultimately, a region corresponding to 60% contribution from the desired species (Figure 5c, shaded regions) was selected. Effectively, this means that the observed KIE will be only 20% of the actual KIE (see Supporting Information for details), which makes for a very challenging measurement. Nonetheless, the enhanced precision of measuring the KIE in a single competitive assay appears to outweigh the challenges; TRESI-based experiments in which the labeled and unlabeled rates were measured separately failed to yield a reliable KIE (i.e., the measurement error was greater than the measurement; data not shown).

Extracted ion currents (XICs) from the appropriate regions of the m/z peaks yield intensity−time profiles dominated by either ^{12}C- or ^{13}C-acylated chymotrypsin as described above (also see methods and Figure S2, Supporting Information). After normalization to the total ion current (TIC) to remove artifacts from sensitivity drift, and averaging over all m/z peaks with sufficient signal-to-noise, we obtain low-dispersion kinetic profiles, an example of which is shown in Figure 6a. To ensure that the observed small rate difference was not the result of systematically changing peak shape or interference from nearby peaks, we performed control experiments in which an identical procedure was used to generate "left-side-of-peak" and "right-side-of-peak" kinetic profiles from samples containing only unlabeled substrate, shown in Figure 6b. These control profiles were identical to within error.

Least-squares fits to the data using a single exponential expression yielded an average ^{12}C acylation rate of 1.10 ± 0.21 s^{-1} and an average ^{13}C acylation rate of 1.06 ± 0.19 s^{-1}, based on five independent runs. The error associated with these independent measurements is too great to allow for the extraction of a reliable KIE; however, this is largely a consequence of run-to-run variability in the absolute rates. Since in a competition experiment KIEs are calculated from *matched* rates (i.e., paired ^{12}C and ^{13}C rates extracted from individual runs), the issue of run-to-run variability is eliminated, resulting in a substantial decrease in the error. After adjusting for peak overlap, the average KIE derived from these

dx.doi.org/10.1021/ac400191t | *Anal. Chem.* 2013, 85, 3758−3764

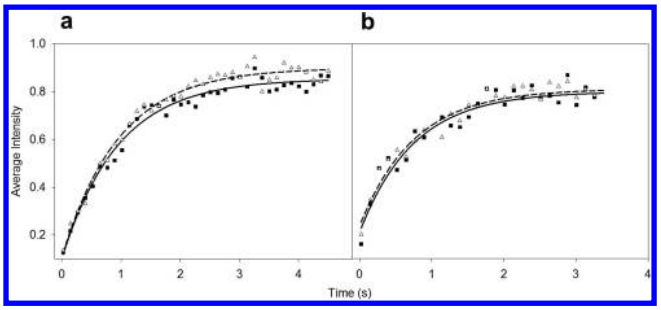

Figure 6. Intensity−time profiles drawn from acyl-chymotrypsin ion currents extracted as shown in Figure 4. Filled squares represent intensities taken from the right side of the peak; open triangles correspond to the intensity on the left side. (a) A typical $^{12}C/^{13}C$ profile for KIE measurement yielding an intrinsic acylation KIE_{obs} of 1.017 ± 0.008, which is 20% of the actual value due to peak overlap (details on the data analysis are provided in the Supporting Information). (b) A $^{12}C/^{12}C$ negative control to ensure that KIE measurements are not an artifact from time-dependent changes in peak shape. The data are fit using least-squares to a single exponential expression yielding a "KIE" of 1.00 ± 0.005.

experiments (n = 5) is 1.09 ± 0.02. To the best of our knowledge, this represents the first competitive heavy-atom KIE measurement in the presteady state. While there are no directly comparable measurements in the literature, this value is within the range determined for deacylation of chymotrypsin using a single-turnover approach (≤1.08, depending on ethanol concentration).[41] The value is significantly higher than the 1.030 ± 0.002 steady state $^{13}(V/K)$ value reported by Hess and co-workers;[40] however, that measurement would have been a convolution of the primary KIEs for acylation and deacylation and would also have been influenced by any change in the ratio of the acylation/deacylation rates resulting from isotopic substitution. The magnitude of our acylation-specific KIE measurement indicates a late transition state for loss of para-nitrophenolate from the tetrahedral acyl-enzyme complex, consistent with strong stabilization of the oxyanion.

CONCLUSIONS

We have demonstrated a novel TRESI-MS-based approach for the measurement of kinetic isotope effects in enzyme catalyzed reactions. The main advantage of TRESI-MS in this context is that is allows for competition experiments in a broad range of systems without the need for radioactive labeling or large amounts of material. Interpretation of the data may also be simplified in many cases, particularly when an enzyme complex is directly observable. Finally, by enabling competition experiments in the presteady state, TRESI-MS greatly increases the number of enzymatic reactions in which it is possible to measure microscopic KIEs (i.e., KIEs that are attributable to a single step in the reaction mechanism). The competition approach was found to be essential in achieving the necessary level of precision for heavy atom KIE measurements. In summary, TRESI-MS represents a powerful alternative for measuring KIEs, with the potential to yield new insights into enzymatic mechanisms, transition states, and catalysis-linked dynamics.

ASSOCIATED CONTENT

Supporting Information

Raw ESI mass spectrum of native YADH (Figure S1). Data acquisition and handling procedure (Figure S2). Data analysis details. This material is available free of charge via the Internet at http://pubs.acs.org.

AUTHOR INFORMATION

Corresponding Author

*Phone: +1 416-736-2100 x 20786. E-mail: dkwilson@yorku.ca.

Present Address

§E.O.-M.: Samuel Lunenfeld Research Institute, Mount Sinai Hospital, 60 Murray St., Toronto, ON, Canada M5G 1X5.

Notes

The authors declare no competing financial interest.

ACKNOWLEDGMENTS

This work was supported by the Natural Sciences and Engineering Council of Canada (NSERC) Discovery Grant program and an Ontario Ministry of Research and Innovation Early Researcher Award.

REFERENCES

(1) Northrop, D. B. *Methods* **2001**, *24*, 117−124.
(2) Mahler, H. R.; Douglas, J. *J. Am. Chem. Soc.* **1957**, *79*, 1159−1166.
(3) Whittaker, M. M.; Ballou, D. P.; Whittaker, J. W. *Biochemistry* **1998**, *37*, 8426−8436.
(4) Papajak, E.; Kwiecien, R. A.; Rudzinski, J.; Sicinska, D.; Kaminski, R.; Szatkowski, L.; Kurihara, T.; Esaki, N.; Paneth, P. *Biochemistry* **2006**, *45*, 6012−6017.
(5) Nesheim, J. C.; Lipscomb, J. D. *Biochemistry* **1996**, *35*, 10240−10247.
(6) Rendina, A. R.; Hermes, J. D.; Cleland, W. W. *Biochemistry* **1984**, *23*, 6257−6262.
(7) Kim, K. H.; Isin, E. M.; Yun, C. H.; Kim, D. H.; Guengerich, F. P. *FEBS J.* **2006**, *273*, 2223−2231.
(8) Knapp, M. J.; Klinman, J. P. *Eur. J. Biochem.* **2002**, *269*, 3113−3121.
(9) Sikorski, R. S.; Wang, L.; Markham, K. A.; Rajagopalan, P. T. R.; Benkovic, S. J.; Kohen, A. *J. Am. Chem. Soc.* **2004**, *126*, 4778−4779.
(10) Hay, S.; Sutcliffe, M. J.; Scrutton, N. S. *Proc. Natl. Acad. Sci. U. S. A.* **2007**, *104*, 507−512.
(11) Swanwick, R. S.; Maglia, G.; Tey, L.; Allemann, R. K. *Biochem. J.* **2006**, *394*, 259−265.
(12) Schramm, V. L.; Horensteins, B. A.; Kline, P. C. *J. Biol. Chem.* **1994**, *269*, 18259−18262.
(13) Schramm, V. L. *Curr. Opin. Struct. Biol.* **2005**, *15*, 604−613.
(14) Berti, P. J. *Methods Enzymol.* **1999**, *308*, 355−397.
(15) Northrop, D. B. *Biochemistry* **1975**, *14*, 2644−2651.
(16) Glowacki, D. R.; Harvey, J. N.; Mulholland, A. J. *Biochem. Soc. Trans.* **2012**, *40*, 515−521.
(17) McCann, J. A. B.; Berti, P. J. *J. Am. Chem. Soc.* **2007**, *129*, 7055−7064.
(18) Kohen, A. *Prog. React. Kinet. Mech.* **2003**, *28*, 119−156.
(19) Sutcliffe, M. J.; Masgrau, L.; Roujeinikova, A.; Johannissen, L. O.; Hothi, P.; Basran, J.; Ranaghan, K. E.; Mulholland, A. J.; Leys, D.; Scrutton, N. S. *Philos. Trans. R. Soc., B: Biol. Sci.* **2006**, *361*, 1375−1386.
(20) Klinman, J. P. *Biochemistry* **1976**, *15*, 2018−2026.
(21) Bates, C.; Kendrick, Z.; McDonald, N.; Kline, P. C. *Phytochemistry* **2006**, *67*, 5−12.
(22) Hunt, C.; Gillani, N.; Farone, A.; Rezaei, M.; Kline, P. C. *BBA-Proteins Proteomics* **2005**, *1751*, 140−149.
(23) Brecker, L.; Kogl, M. F.; Tyl, C. E.; Kratzer, R.; Nidetzky, B. *Tetrahedron Lett.* **2006**, *47*, 4045−4049.
(24) Chan, J.; Lewis, A. R.; Gilbert, M.; Karwaski, M. F.; Bennet, A. J. *Nat. Chem. Biol.* **2010**, *6*, 405−407.

(25) Singleton, D. A.; Thomas, A. A. *J. Am. Chem. Soc.* **1995**, *117*, 9357−9358.
(26) Werner, R. A.; Brand, W. A. *Rapid Commun. Mass Spectrom.* **2001**, *15*, 501−519.
(27) Wilson, D. J.; Konermann, L. *Anal. Chem.* **2003**, *75*, 6408−6414.
(28) Wilson, D. J.; Konermann, L. *Anal. Chem.* **2004**, *76*, 2537−2543.
(29) Powell, M. F.; Bruice, T. C. *J. Am. Chem. Soc.* **1983**, *105*, 7139−7149.
(30) Northrop, D. B.; Cho, Y. K. *Biochemistry* **2000**, *39*, 2406−2412.
(31) Cha, Y.; Murray, C. J.; Klinman, J. P. *Science* **1989**, *243*, 1325−1330.
(32) Bahnson, B. J.; Colby, T. D.; Chin, J. K.; Goldstein, B. M.; Klinman, J. P. *Proc. Natl. Acad. Sci. U. S. A.* **1997**, *94*, 12797−12802.
(33) Kohen, A.; Cannio, R.; Bartolucci, S.; Klinman, J. P. *Nature* **1999**, *399*, 496−499.
(34) Hay, S.; Johannissen, L. O.; Hothi, P.; Sutcliffe, M. J.; Scrutton, N. S. *J. Am. Chem. Soc.* **2012**, *134*, 9749−54.
(35) Dickinson, F. M.; Monger, G. P. *Biochem. J.* **1973**, *131*, 261−270.
(36) Zhang, H.; Cui, W. D.; Wen, J. Z.; Blankenship, R. E.; Gross, M. L. *J. Am. Soc. Mass Spectrom.* **2010**, *21*, 1966−1968.
(37) Loo, J. A. *J. Mass Spectrom.* **1995**, *30*, 180−183.
(38) Klinman, J. P. *J. Biol. Chem.* **1972**, *247*, 7977−7987.
(39) Park, H.; Kidman, G.; Northrop, D. B. *Arch. Biochem. Biophys.* **2005**, *433*, 335−340.
(40) Hess, R. A.; Hengge, A. C.; Cleland, W. W. *J. Am. Chem. Soc.* **1998**, *120*, 2703−2709.
(41) Mishra, A. K.; Klapper, M. H. *Biochemistry* **1986**, *25*, 7328−7336.